

Columnar architected thin films – deposition, microstructure and related properties*

N. STARBOV*, K. STARBOVA

*Central Laboratory of Photoprocesses “Acad. J. Malinowski”, Bulgarian Academy of Sciences
Acad. Georgi Bonchev Str., Block 109, 1113 Sofia, Bulgaria.*

A great variety of inorganic and organic thin films are deposited via Joule heating- or electron beam-evaporation in high vacuum. It is shown that in a proper range of basic deposition parameters such as substrate temperature, deposition rate and vapor incidence angle, thin films with micro- or nano-sized surface features and column-like internal structure can be grown. Column inclination toward the substrate plane, as well as a pronounced anisotropy of the column cross section at high vapor incidence angles is established. The revealed internal film structure is found to influence the microhardness, thermal diffusivity, DC-electric conductivity and effective refractive index, by inducing in-plane anisotropy. This is most pronounced at high vapor incidence angles, which is explained by specific morphological features of the films studied. Our results confirm the occurrence of general columnar growth phenomena based on a simple physical self-shadowing mechanism of the ad-species during the early and advanced stages of thin film deposition. Finally, the advantage of the glancing angle deposition technique is discussed as an opportunity for the versatile fabrication of micro- and nano-porous coatings with high specific surface suitable for a large spectrum of applications in catalysis, sensor technology, biomedical engineering etc.

(Received November 5, 2008; accepted December 15, 2008)

Keywords: Obliquely deposited thin films, Microstructure, Physical properties, Applications

1. Introduction

A great number of innovative R & D activities in the field of catalysis, sensor techniques, electrochemistry and biomedical engineering are based on processes which occur at the solid surfaces or interfaces. Thin solid films are widely used as functional materials of great importance in these fields of technological interest. The practical realization of the micro- and nano-sized materials is determined by their specific mechanical, thermal, electrical and optical properties. Recently, porous thin films with high specific surface have been applied as active components in absorbers [1], membranes for separation and purification of liquids and gases [2], catalysts for oxidation and reduction of pollutive gases from the chemical industry, and automotive engines ([3-5] etc.) Porous oxides and other ceramic materials with high surface-to-volume ratio are used as active media for monitoring and controlling the pressure, humidity or pollutive gases in the environment [6,7].

Usually the vacuum deposited thin films possess relatively smooth surfaces, with features on the micron scale. This imposes the application of post-deposition techniques like physical, chemical or electrochemical etching, laser roughening, etc. for preparation of porous films with high specific surface. The only “ad-initium”

method for the coating of thin films with high porosity, is “glancing angle deposition”. The principle of this elegant technique is based on collimated material flux impinging on the substrate under an oblique “incidence angle”. As a result, porous thin films with a columnar microstructure and a high surface-to-volume ratio could be produced.

The aim of the present paper is to demonstrate the efficacy of the oblique deposition for preparation of different porous thin films and to represent their microstructure related properties, as well as to point out some applications of these micro- and nano-sized materials.

2. Experimental

Fig. 1 illustrates the principle of the oblique vacuum deposition of thin films, where α is the vapor incidence angle between the material flux and the substrate normal. The same scheme could be presented for illustration of the electrochemical deposition of metal coatings, the arrangement of the substrate and the ion flux being designed on the base of the Hull cell [8]. As seen from the figure, the vapor incidence plane is defined by the flux direction and its projection onto the substrate surface. For simplicity, we shall further operate with the definitions

* Paper presented at the International School on Condensed Matter Physics, Varna, Bulgaria, September 2008

“parallel” or “perpendicular” to that plane marking the corresponding indices in the text, and in graphs with “||” or “ \perp ”.

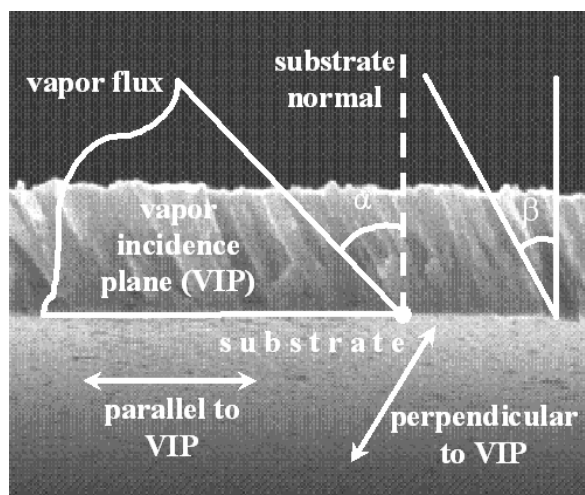


Fig.1. Principal scheme of vacuum deposited thin films with columnar structure: VIP- vapor incidence plane, α – vapor incidence angle, β – column inclination towards the substrate surface.

Standard high vacuum systems were used for sample preparation. The majority of materials were thermally evaporated from indirectly heated Knudsen vessels. The refractory oxides were e-gun deposited through an appropriate diaphragm, making use of only that part of the vapor flux which is normal to the target surface. Carefully pre-cleaned soda-lime-glass served as substrates, stainless steel plates being used for the electrochemical deposition of metals only. The vapor incidence angles α was varied from 0° to 80° , via orientation of the substrate normal toward the flux direction. All samples were prepared under ambient conditions at a constant deposition rate in the range 0.1 to 1.0 nm/s, and a background pressure of the order of 5.0×10^{-4} Pa. Thus, 1.0 to 4.0 μm thick films were produced by varying the deposition time only.

Measurements of the microstructure related properties of the films studied are described in detail elsewhere [9,10]. Here the experimental methods used will be mentioned only briefly. The microhardness ($Mh_{||}$ or Mh_{\perp}) was evaluated from long edge indentation of the Knoop prism, at a constant indenter loading between 1.5 and 10 g, dependent on the material hardness. The DC electrical conductivity was measured parallel or perpendicular to the vapor incidence plane ($\sigma_{||}$ or σ_{\perp}), by means of a precise Wheatstone bridge ($10 - 10^8 \Omega$). In the range $10^8 - 10^{12} \Omega$, the resistance evaluation was made via voltage drop measurements after applying a standard voltage of 1 V to the sample connected in a series with a precision resistor. The optical properties of the films were followed by recording the optical transmittance (T), by means of a Carry 5 UV-VIS-NIR spectrophotometer, in the wavelength range 200-1500 nm. Linearly polarized light was used to align the plane of polarization parallel or

perpendicular to the vapor incidence plane. The effective refractive index in both directions ($n_{||}$ or n_{\perp}) was evaluated on the basis of the mini-max envelope of the T-spectra beyond the absorption edge, using Swanepoel's method [11] and a developed computer program [12]. The thin film growth morphology was imaged and recorded using a Phillips 515 Scanning Electron Microscope (SEM). A standard microfractographic technique was applied for preparing thin film growth profiles for SEM observation. Special precautions were taken for the cutting procedure to be performed as precisely as possible perpendicular to the vapour incidence plane [13]. Furthermore, thin conductive carbon and gold coatings were consecutively deposited on the examined top film surfaces and growth profiles, thus providing SEM imaging under the most favourable resolution conditions.

3. Results

Fig. 2 demonstrates the surface morphology and growth profile of an Ag_2S sample which is typical of thin films prepared via obliquely vapor deposition. It is obvious that the Ag_2S film grows in a columnar fashion.

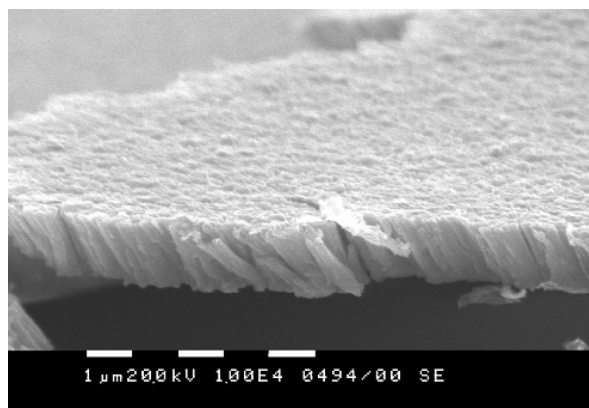


Fig.2. SEM micrograph of a crystalline Ag_2S thin film deposited at $\alpha=45^\circ$. SEI mode.

The individual closely packed columns run through the entire film thickness. The film free surface was granular, the mean grain size being commensurate with the column mean cross-section.

The evolution of the internal film microstructure when α rises is illustrated in Fig.3 for amorphous ZrO_2 . It is clearly seen that the column inclination β towards the substrate surface increases with the incidence angle α . Usually, at α values higher than 40° , the columns are separated from low density material and the free volume. When α is $\geq 60^\circ$, transformation of the latter into pores through the entire film thickness takes place. This drastic change in the film growth morphology is accompanied by the formation of coarse, ordered surface morphology, as

shown in Fig. 4 for both amorphous As_2S_3 and crystalline AgBr thin films.

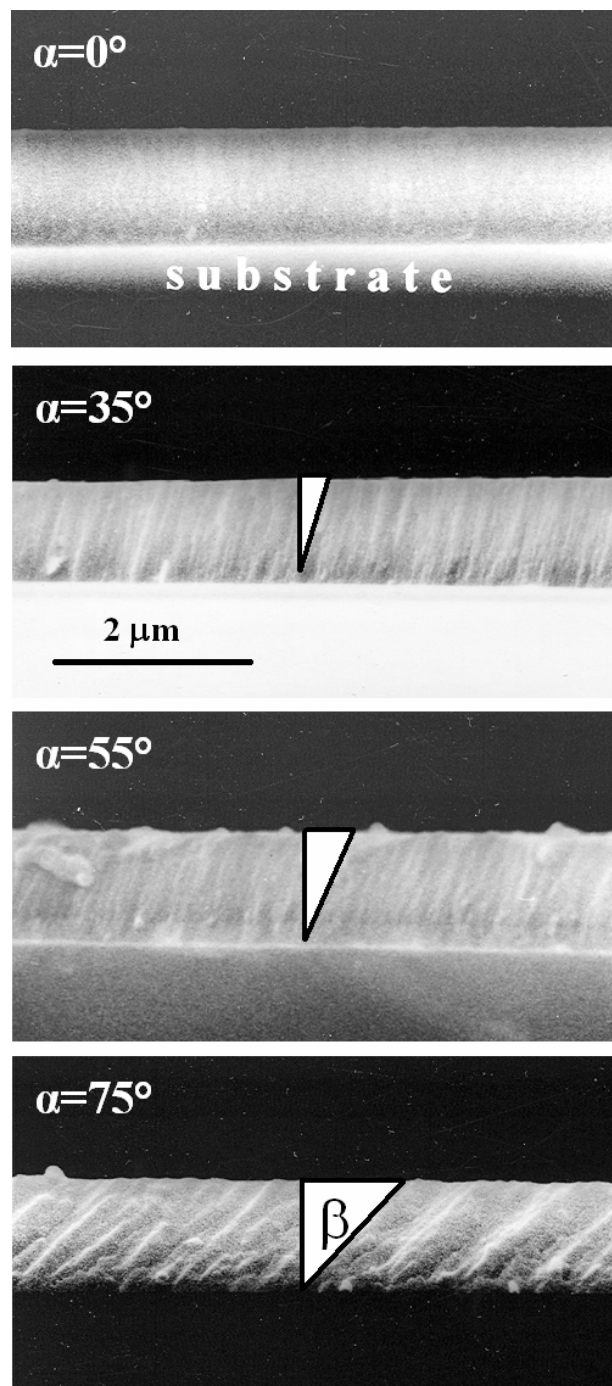


Fig.3. SEM micrographs of the growth profiles of ZrO_2 films deposited at different vapor incidence angles, α .

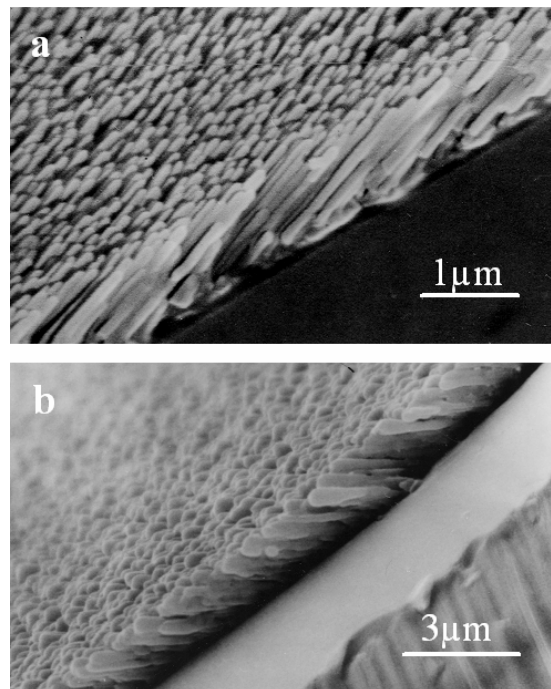


Fig.4. SEM micrographs of: (a) - amorphous As_2S_3 and (b) - a crystalline AgBr thin film deposited at $\alpha=80^\circ$. SEI, tilt angle (a) - 45° and (b) - 40° .

Here, one should remember the existence of correlation between the angles of vapour incidence α and the column inclination β , empirically formulated by Nieuwenhuizen and Haanstra [13] as:

$$\text{tg} \alpha = 2 \text{tg} \beta \quad (1)$$

This so called “tangent rule” is satisfied for a great number of amorphous as well as crystalline thin films, as summarized in Fig. 5 [14]. The β -values for obliquely deposited crystalline AgBr [15,16], AgCl [17], Ag_2S [18,19], Sb_2Se_3 [20], or amorphous - As_2S_3 [9,21], GeS_2 [10], ZrO_2 [22] and Al_2O_3 [23] are inserted in this figure as well. As can be seen, the results obtained in our laboratory also obey the relation (1).

The film microstructure strongly influences the physical properties of the samples studied. Fig.6. presents some examples showing that the microhardness M_h , DC-conductivity σ and refractive index n are monotonically decreasing functions of α . A similar dependence on α is also observed for the thermal diffusivity κ of a- Al_2O_3 films [23], which is very useful, when the film resistance is extremely high [24].

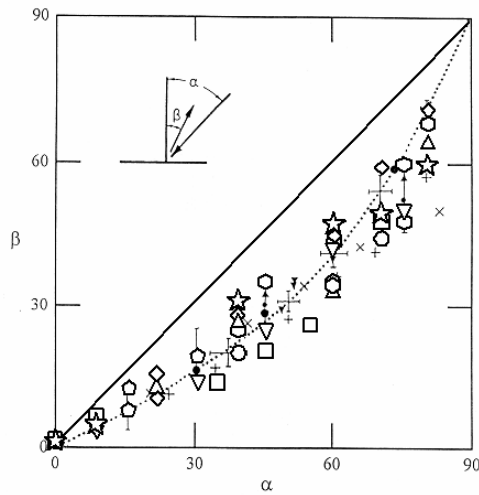


Fig. 5. Column inclination β as dependent on the vapor incidence angle α , as published in [14], for various thin films – black symbols relate to the films studied: \circ a - Al_2O_3 , \square a - ZrO_2 , Δ a - GeS_2 , \diamond a - As_2S_3 , ∇ c - Sb_2Se_3 , ∇ c - $AgCl$, \star c - $AgBr$ and \hexagon c - Ag_2S .

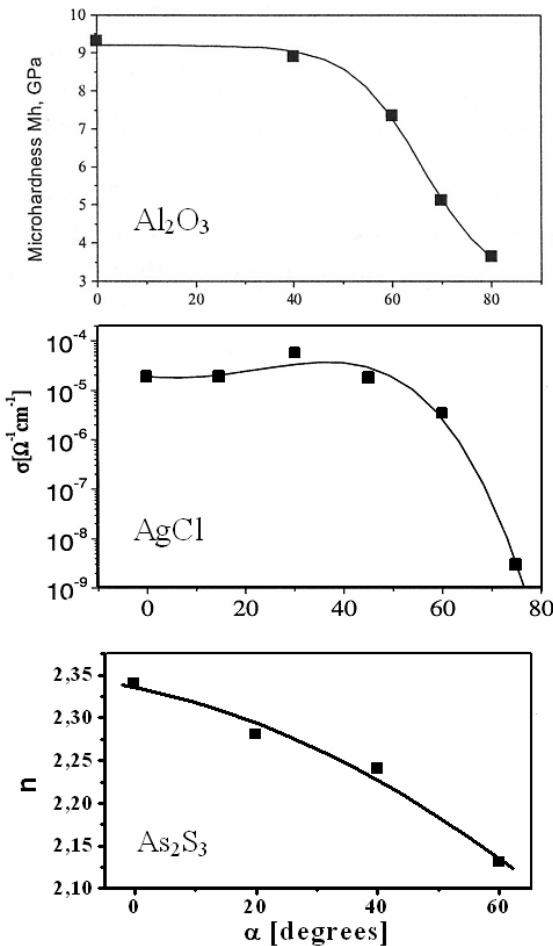


Fig. 6. M_h , σ and n , as dependent on α .

Furthermore, it is found that the revealed columnar microstructure also influences the basic physical properties, by inducing in-plane anisotropy, which is most pronounced at high vapour incidence angles (Fig. 7). The different values, measured parallel or normal to the vapor

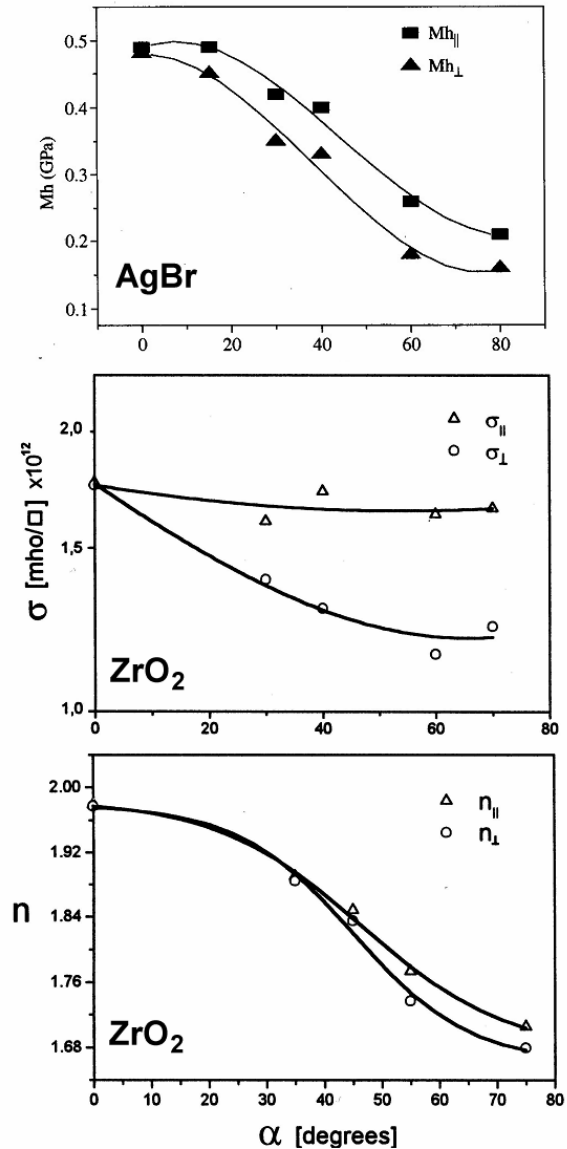


Fig. 7. The microhardness $M_{h\parallel}$ or $M_{h\perp}$, the DC-conductivity per unit surface σ_{\parallel} or σ_{\perp} , as well as the refractive index n_{\parallel} or n_{\perp} at $\lambda=600$ nm, as dependent on α .

incidence plane is related to the different column shapes observed in obliquely deposited films, as compared to samples obtained at $\alpha=0^\circ$. Fig. 8. demonstrates the columns' cross-section transformation from circular at $\alpha=0^\circ$ into elongated and close to elliptical ones when α rises, the long axes being normal to the vapor incidence plane.

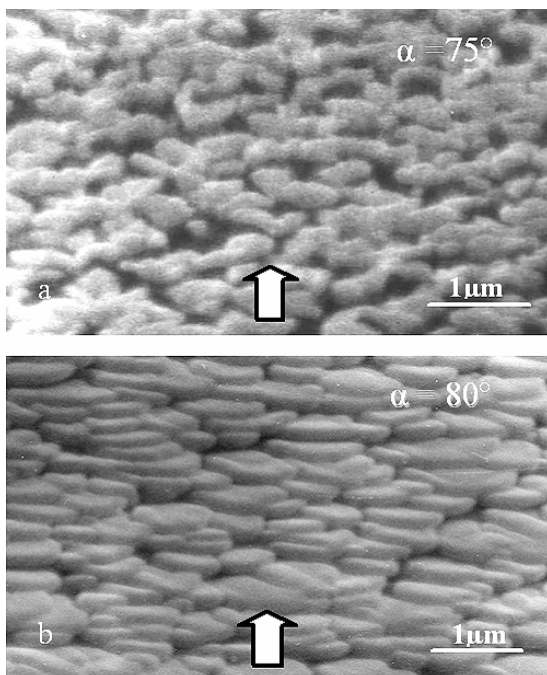


Fig. 8. SEM micrographs of the top surface of: (a) crystalline Ag_2S and (b) amorphous As_2S_3 thin films deposited at high vapor incidence angles. The arrows indicate the vapor flux incidence. SEI, tilt angle (a) - 50° and (b) - 60° .

It should be noted that the deposition parameters listed above as the: deposition rate, residual pressure, substrate temperature etc., are not always optimal for the preparation of columnar architected thin films. For example, Se grows under these deposition conditions as amorphous films, which are structureless on microscopic scale. The lack of success in this case is due to the very high vapor pressure of Se under high vacuum conditions, which hinders any effort to collimate the selenium vapor flux. Additionally, Se adatoms possess a very high mobility either on the glass substrate surface or onto the selenium deposited after condensation of the first discontinuous Se

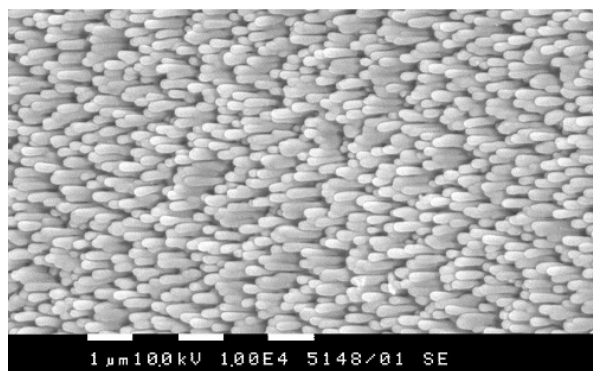


Fig.9. SEM micrographs of the top surface of an amorphous Se thin film deposited at $\alpha = 80^\circ$. SEI – tilt angle 40° .

layer. However, it is possible to obtain Se films with a columnar microstructure under proper deposition conditions, which are carefully selected in order to overcome the mentioned difficulties [25]. Fig. 9 demonstrate that Se films could be prepared in the same fashion as the columnar structured amorphous and crystalline materials presented in this paper. It should be mentioned, here, that the value $\beta=65^\circ$, as obtained for these samples, satisfies well the tangent rule.

Finally, the oblique deposition could be applied by every method, which allows one to form a collimated material flux oriented under a definite angle toward the substrate normal. The overall validity of this approach could be demonstrated by electrochemical metal deposition. Fig. 10 represents a thin film of crystalline Ni, deposited

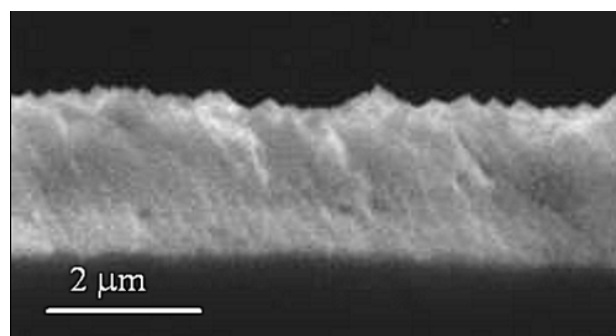


Fig.10. SEM micrograph of the growth profile of an electrochemically coated Ni film at $\alpha = 60^\circ$.

onto a glass substrate coated with ITO [26]. It was prepared using a modified Hull cell [8], the metal ion flux being inclined with respect to the cathode surface. Thus, Ni films with thicknesses between 2 and 3 μm could be deposited for 1 hour at current densities of about 2-3 A/cm^2 , the electrolyte being a conventional Watson sulphamate Ni-bath at 25°C [27]. As seen in Fig. 10, the columnar microstructure of the Ni film is also resolved, the low image contrast being probably due to the nano-sized dimensions of the columnar cross section.

4. Discussion

The microstructure of obliquely deposited thin films, as revealed under a scanning electron microscope, shows practically the same morphological features. Obviously, the columnar growth is typical for all materials studied, although different deposition methods or substrates are used and specific preparation conditions sometimes have to be selected. This means that the oblique deposition is controlled by a simple physical principle, formulated by Dirks and Leamy [14]. It is known as a “self shadowing mechanism” of thin film growth, when the material flux impinges on the substrate surface at an angle $\alpha \neq 0^\circ$. In this case, the initially formed nuclei after adsorption of the first atoms or molecules shadows the space behind the growing cluster from the next impinging species. Thus, low density

material is formed in the shadowed part of the substrate and the cluster grows predominantly in the direction of material flux. As a result, the deposited film grows in columnar fashion, with a closely packed microstructure at small vapor incidence angles or a porous one when α exceeds 60° . It is clear that the column cross section depends on the initial number of nuclei formed. At high supersaturation and a great number of specific (for every substrate material) adsorption sites, columns with nano-sized dimensions will grow, as in the case of ZrO_2 thin films (Fig. 3.). Otherwise, large columns with cross sections increased by up to a hundred nanometers will be formed. Pores with the same dimensions are typical for films with similar microstructures (Fig.4, Fig.9). Of course, the mobility of atoms or molecules on the substrate or on the surface and in the bulk of the grown film has to be low enough to preserve the columns' habit. This requirement is satisfied for a low substrate temperature, plus a limited mobility of the ad-species on both the substrate and deposited film of the selected material. Obviously, the columnar microstructure of the obliquely deposited crystalline or amorphous materials is a result of the occurrence of general nucleation and thin film growth phenomena.

As seen in Fig. 5, even for the data selected by Dirks and Laemy from the literature [14], the tangent rule (1) is not always strictly satisfied. In our experiments, the calculated experimental error was $\pm 5\%$, but it could exceed 20% if the microfractographic procedure is not carefully carried out. In particular, the deviation from (1) at $\alpha > 60^\circ$ is the reason why some authors have criticized the tangent rule as "not universally valid". There are several theoretical models which try to find alternative dependences between the vapor incidence angle α and the column inclination β . However, the most relevant to the experiments is the assumption of Krug [28] that different densities of the films deposited at various vapor incidence angles plays a crucial role in the β vs. α relationship. Thus, a new relation based on the angular dependence of the film density $\rho(\alpha)$ is developed:

$$\operatorname{tg} \beta = \operatorname{tg} \alpha + \frac{\rho'(\alpha)}{\rho(\alpha)} \quad (2)$$

where $\rho'(\alpha)$ is the first derivative of the film density $d\rho/d\alpha$ [28]. The result of a numerical calculation of β , according to (2), is presented in Fig.11. Since $\rho(\alpha)$ is a decreasing function of α , the measured column inclination β has to be substantially smaller than that predicted by eq. (1). To the best of our knowledge, however, until now the relation (2) has not been verified by experiment.

In our opinion, there is another explanation of the fact that the tangent rule (1) seems not always to be satisfied. Looking at Fig. 1, simple geometrical considerations indicate that the column inclination β has its maximal value in the vapor incidence plane. This means that β will always be smaller when the prepared microfractographic profile does not coincide with this plane. It is obvious that when the film profile is prepared perpendicular to the vapor incidence plane, "straight" columns parallel to the

substrate normal will be visualized by conventional SEM observations. However, except for experimental experience, the perfection of the sample profiles depends on the hardness of the deposited materials, as well as on the fractographic properties of the substrate used. Therefore, the experimental error observed in several cases could be very high. It should be noted, here, that the tangent rule is very useful for evaluation of the material flux collimation, if large scale obliquely deposited films have to be prepared from only one source. Additionally, a conclusion for the reaction location could be made via verification of eq. (1) when two or more separate vapor sources are used for co-deposition of films with binary or ternary compositions. Thus, it is established that the synthesis of silver sulfide during the preparation of Ag_2S by co-evaporation of Ag and S occurs at the substrate surface [18,19].

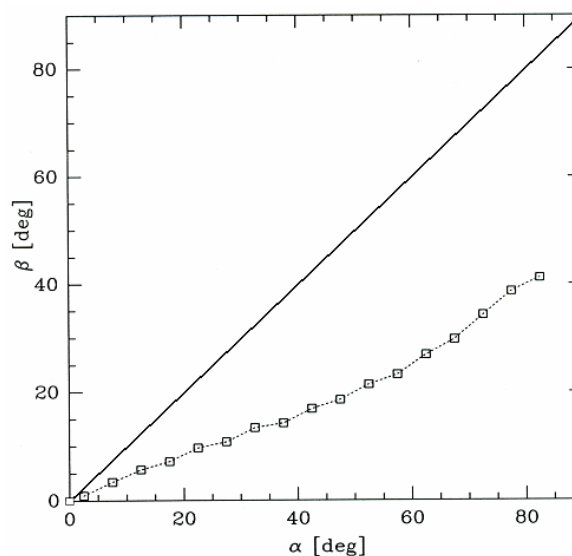


Fig.11. Column inclination β vs. α as follows from equation (2) and as published in [28].

The results in the present study reveal basic relationships between the film microstructure and the microhardness M_h , DC-conductivity σ , thermal diffusivity κ , as well as the refractive index n . The M_h , σ , κ and n values drop substantially when α increases above 60° , since the relative amount of low density material or free volume between the individual columns rises substantially. This influence of the vapor incidence angle is more pronounced in σ which, as known, is the most sensitive material parameter to the changes of the material microstructure. Also, the oblique deposition induces an optical inhomogeneity at $\alpha > 40^\circ$. The light scattering from the inter-columnar boundaries is so strong that the films look opaque in visible light if the vapor incidence angle is higher than 60° . In some cases, as for example for $AgCl$ films [17], the calculation of the effective refractive index n is impossible, since the optical transmittance drops to

zero. The similarity in the physical properties are obviously due the occurrence of general growth mechanism of the columnar structured thin films.

The column shape anisotropy visualized at $\alpha > 60^\circ$ results, as predicted by Macleod [29], in anisotropy of the values measured parallel and perpendicular to the vapor incidence angle. It is evident from Fig. 8 that the Knoop prism should remove and push aside more “closely packed” material if the prism long edge is oriented in the direction parallel to the vapour incidence plane. Thus, Mh_{\parallel} values exceed those of Mh_{\perp} (Fig. 7). Usually, the values of σ_{\parallel} are also higher than those of σ_{\perp} , as shown in Fig. 6. One can suppose that the in-plane anisotropy and related asymmetrical distribution of the contacts between individual columns produce specific electrical networks. Thus, the current carriers should pass through a longer pathway in a direction perpendicular to the vapor incidence plane than in a direction parallel to that plane. The electrical transport is additionally complicated when the film material is characterized with a surface conductivity substantially higher than that in the bulk, which is typical of silver halides [30]. In this case, the surface-to-volume ratio of the columns increases with α and the ionic transport occurs predominantly in the vicinity of the column surface. It is clear that the overall electrical transport should be a combination of the ionic motion within columns and ion transfer along and through the contacts between the individual columns. As a result of this competition, the ionic carriers should pass through a longer pathway between the electrodes in the direction parallel to the vapor incidence plane than in the direction normal to that plane. Thus, σ_{\parallel} has to be smaller than σ_{\perp} , which is observed in obliquely deposited AgBr thin films at $\alpha > 40^\circ$ [16].

The films' optical inhomogeneity mentioned above is also accompanied with in-plane anisotropy of the refractive index of the samples. The light propagation in the direction perpendicular to the vapor incidence plane is higher, and for a given α and wavelength λ , n_{\perp} always has smaller values than n_{\parallel} . In this case, the presence of intrinsic birefringence $\Delta n = (n_{\parallel} - n_{\perp})$ in obliquely deposited films is revealed. For ZrO₂ films (Fig. 7.) Δn ranges between 0.01 and 0.08 when α rises from 35° to 75° [22].

Summarizing the results presented, it is obvious that the basic physical properties of the columnar structured thin films could be deliberately and purposefully modified by varying only one deposition parameter – the flux incidence angle α . Oblique deposition reveals great and unemployed potential for innovative R & D activity in the field of materials science. This method is simple, versatile and could be applied to every deposition technique, which allows the alignment of a collimated material flux for thin film preparation. For example, the fabrication of films with a high porosity is of great importance, especially for those processes which are related to the amount of adsorbed gases and liquids. The high surface-to-volume ratio of functional materials, as used in the field of catalysis or sensor techniques, results in a greater efficiency of the catalytic process and detection sensitivity

of the sensor. Our efforts to develop more efficient sensors for hazardous ionophilic gases show that this approach is very successful. The specific surface of the obliquely deposited at $\alpha = 60^\circ$ AgCl films is only fourfold larger than that of films deposited at $\alpha = 0^\circ$. However, this increased surface-to-volume ratio results in an 8 – 10 times higher relative sensitivity for the detection of ammonia or dimethylamine vapors [31].

The opportunity for optical application of the columnar architected thin films is also very attractive. Recently, the research team of Fujifilm Co. developed a new X-ray focusing detector plate for radiographic diagnostics [32]. The plate is covered with a columnar microstructured phosphor material, the columns being effective light guides of X-radiation. This increases by factor of two the quantum efficiency of the imaging plate in the radiographic equipment, thus reducing substantially the irradiation dose of the examined patients. A lot of applications of columnar architected thin films are outlined also in optoelectronic R & D, for the production of optical elements such as tunable laser mirrors, narrow pass-band or rugate-like filters, as well as devices such as optical sensors, linear and non-linear optical circuits, sculptured nematic thin films, liquid crystal devices, etc. [33].

5. Conclusions

The present paper demonstrates the universality of oblique deposition for the preparation of columnar architected thin films from different amorphous and crystalline materials. It is shown that this deposition technique could be always realized, provided the material flux is aligned towards the substrate surface at a definite incidence angle. Thus, functional materials with proper basic physical properties could be developed for a wide field of practical applications. It is the author's deep belief that oblique deposition could be also applied for the preparation of many organic materials which will offer novel R&D activity in biochemical and biomedical engineering.

Acknowledgements

This paper could not have been completed without close collaboration with our colleagues and co-workers Dr. B. Mednikarov, Dr. J. Dikova, Dr. V. Mankov, Dr. D. Krashanova, Dr. M. Levichkova, Mr. E. Krumov and Mrs. R. Georgieva, as well as Mr. D. Popov – Institute of Physical Chemistry, Bulgarian Academy of Sciences.

References

- [1] D. E. Fain, MRS Bull. **19**, 40 (1994).
- [2] R. R. Brave, Inorganic Membranes: Synthesis, Characteristics and Applications, Van Nostrand Reinhold, New York (1991).

- [3] J. Woestman, E. Logothetis, *Industrial Physicist* **11/12**, 20 (1995).
- [4] A. Baiker, *Chimia* **50**, 65 (1996).
- [5] Z. Zulkarnian, L. K. Hui, M. Z. Hussein, Y. H. Taufiq-Yap, A. H. Abdullah, I. Ramli, J. Hazard. Mater. **B125**, 113 (2005).
- [6] A. Cybulski, J. A. Moulijn, in „Structured Catalysts and Reactors“, Eds. A. Cybulski and J. A. Moulijn, Marcel Dekker Inc., New-York-Basel-Hong Kong (1998), p.1.
- [7] J. A. Schwarz, C. Contescu, A. Contescu, *Chem. Rev.* **95**, 477 (1995).
- [8] D. R. Gabe, G. D. Wilcox, *Trans. Inst. Metal Finish.* **71**, 71 (1993).
- [9] N. Starbov, K. Starbova, J. Dikova, *J. Non-Cryst. Solids* **139**, 222 (1992).
- [10] K. Starbova, V. Mankov, J. Dikova, N. Starbov, *Vacuum* **53**, 441 (1999).
- [11] R. Swanepoel, *J. Phys. E* **16**, 1214 (1983).
- [12] I. Konstantinov, unpublished program product.
- [13] J. M. Nieuwenhuizen, H. B. Haanstra, *Phillips Tech. Rev.* **27**, 87 (1966).
- [14] A. G. Dirks, H. J. Leamy, *Thin Solid Films* **47**, 219 (1977).
- [15] R. Georgieva, D. Karashanova, N. Starbov, *Vacuum* **69**, 327 (2003).
- [16] R. Georgieva, D. Karashanova, N. Starbov, *J. Mater. Sci.: Materials in Electronics* **14**, 773 (2003).
- [17] N. Starbov, K. Starbova, *Nanoscience & Nanotechnology Issue* **5**, ed. E. Balabanova and I. Dragieva, Heron Press Ltd., Sofia (2005) p.73.
- [18] D. Karashanova, K. Starbova, N. Starbov, *J. Optoelectron. Adv. Mater.* **4**, 903 (2003).
- [19] D. Karashanova, K. Starbova, N. Starbov, *Nanoscience & Nanotechnology Issue* **4**, ed. E. Balabanova and I. Dragieva, Heron Press Ltd., Sofia (2004) p.293.
- [20] K. Starbova, J. Dikova, V. Mankov, N. Starbov, *Vacuum* **47**, 1487 (1996).
- [21] K. Starbova, J. Dikova, N. Starbov, *J. Non-Cryst. Solids* **210**, 261 (1997).
- [22] M. Levichkova, V. Mankov, N. Starbov, D. Karashanova, B. Mednikarov, K. Starbova, *Surf. Coat. Technol.* **141**, 70 (2001).
- [23] E. Krumov, V. Mankov, K. Starbova, *Vacuum* **76**, 211 (2004).
- [24] E. Krumov, V. Mankov, N. Starbov, *J. Optoelectron. Adv. Mater.* **7**, 2619 (2005).
- [25] K. Starbova, N. Starbov, to be published.
- [26] K. Starbova, D. Popov, N. Starbov, to be published.
- [27] S. A. Watson, *Nickel Sulphamate Solutions*, NiDI Technical Series 10052, Nickel Development Institute, Toronto (1989).
- [28] J. Krug, *Mat.-Wiss. u. Werkstofftech.* **26**, 22 (1995).
- [29] H. A. Macleod, *J. Vac. Sci. Technol.* **A4**, 418 (1986).
- [30] N. Starbov, *J. Inf. Rec. Mater.* **13**, 307 (1985).
- [31] R. Georgieva, N. Starbov, D. Karashanova, K. Starbova, submitted for publication in this issue of *J. Optoelectron. Adv. Mater.*
- [32] Y. Iwabuchi, S. Tazaki, H. Yasuda, A. Takasu, Y. Isoda, M. Kahsiwaya, Y. Hosoi, *Fujifilm Research and Development* **52**, 22 (2007).
- [33] R. Messier, A. Lakhtakia, *Mat. Res. Innovat.* **1**, 145 (1997), *Ibid.* **2**, 217 (1999).

*Corresponding author: nstar@clf.bas.bg